A new zebrafish bone crush injury model

Sara Sousa[1,2], Fabio Valerio[1] and Antonio Jacinto[1,3,*]

[1]Instituto de Medicina Molecular da Faculdade de Medicina da Universidade de Lisboa, 1649-028 Lisboa, Portugal
[2]PhD Programme in Experimental Biology and Biomedicine, (5th PDBEB), Center for Neuroscience and Cell Biology, University of Coimbra, 3004-517 Coimbra, Portugal
[3]CEDOC, Faculdade de Ciências Médicas, Universidade Nova de Lisboa, 1169-056, Lisboa, Portugal
*Author for correspondence (antonio.jacinto@fcm.unl.pt)

Biology Open 1, 915–921
doi: 10.1242/bio.2012877
Received 9th February 2012
Accepted 31st May 2012

Summary

While mammals have a limited capacity to repair bone fractures, zebrafish can completely regenerate amputated bony fin rays. Fin regeneration in teleosts has been studied after partial amputation of the caudal fin, which is not ideal to model human bone fractures because it involves substantial tissue removal, rather than local tissue injury. In this work, we have established a bone crush injury model in zebrafish adult caudal fin, which consists of the precise crush of bony rays with no tissue amputation. Comparing these two injury models, we show that the initial stages of injury response are the same regarding the activation of wound healing molecular markers. However, in the crush assay the expression of the blastema marker *msxb* appears later than during regeneration after amputation. Following the same trend, bone cells deposition and expression of genes involved in skeletogenesis are also delayed. We further show that bone and blood vessel patterning is also affected. Moreover, analysis of *osteopontin* and Tenascin-C reveals that they are expressed at later stages in crushed tissue, suggesting that in this case bone repair is prolonged for longer than in the case of regeneration after amputation. Due to the nature of the trauma inflicted, the crush injury model seems more similar to fracture bone repair in mammals than bony ray amputation. Therefore, the new model that we present here may help to identify the key processes that regulate bone fracture and contribute to improve bone repair in humans.

Key words: Zebrafish, Caudal fin, Epimorphic regeneration, Injury, Crush, Bone

Introduction

In a broad sense, regeneration can be defined as the reconstitution of a lost or injured part. However, such definition encompasses a large range of phenomena that operate through different mechanisms. Classically, the most well described type of regeneration is the epimorphic regeneration, characterized by the formation of a blastema, a mass of less differentiated cells that gives rise to the new structure functionally equivalent to the lost one (Morgan, 1901; Kragl et al., 2009). Although humans and other vertebrates have the ability to repair some tissues and organs, they cannot undergo epimorphic regeneration. For instance, human skeletal tissues undergo a continuous process of bone remodelling to maintain their functional integrity, however, if a more serious injury occurs the process of fracture repair is initiated without the formation of a blastema. In mammals, it is believed that repair of bone fractures is achieved by local activation and differentiation of osteogenic progenitor cells (Maes et al., 2010). This process seems to be quite different from what happens in regeneration models, such as zebrafish where bony fin rays regenerate from mature osteoblasts that dedifferentiate to form a blastema (Knopf et al., 2011; Sousa et al., 2011). Thus, fracture repair in mammals cannot be accurately compared with the epimorphic regenerative process. Nevertheless, zebrafish fins have been extensively used as a model system for skeletal studies mainly due to its remarkable regenerative ability, ease of accebility of the fin and the conservation of signals involved in bone differentiation that are re-activated during the epimorphic regenerative process. In adult zebrafish, the amputation of the caudal fin leads to a succession of steps (wound healing, blastema formation and regenerative outgrowth) that restore the various tissues comprising the fin, including blood vessels, nerves, connective tissue, epidermis, pigment cells and skeletal elements that support the fin structure (Akimenko et al., 2003). Zebrafish fin skeletal elements are actinotrichia and lepidotrichia, the latter ones consist of segmented bony rays, each comprised of concave, facing hemirays. The vascular architecture in the caudal fin is organized with an artery in the middle of each bony ray, veins located on each side of the bony structure and a set of smaller blood vessels form the connecting microvasculature in the inter-ray mesenchyme (Huang et al., 2003). Despite of bone being a highly vascularized tissue, the possible function of angiogenesis in bone regeneration is still poorly defined. However, there is a report in zebrafish suggesting that blood vessels play an important role in the patterning of bony rays in zebrafish caudal fins (Huang et al., 2009).

Moreover, in mammals it is known that the shape of bone changes accordingly with the physical constraints such as mechanical stress (Allori et al., 2008). This change is a result of a bone remodelling process; a tightly coordinated event that requires the synchronized activities of multiple cellular participants to ensure that bone resorption and formation occur

sequentially at the same anatomical location to preserve bone mass (Allori et al., 2008). However, the factor that triggers these sequential cellular events has not been elucidated yet, but some molecules have been described to be involved in this process, such as a major non-collagenous bone matrix protein, Osteopontin and the extracellular matrix protein, Tenascin-C (Mackie, 1994; Denhardt and Guo, 1993).

In the last decade there has been a growing number of studies on zebrafish caudal fin epimorphic regeneration following an amputation (Poss, 2010). However, how fin regeneration proceeds in fracture repair, which involves tissue damage rather than tissue loss or removal has not been addressed. In previous studies either caudal fin tissue is cut off before the first bony ray bifurcation (Laforest et al., 1998) or a single hemiray is removed from the basis of the caudal fin (Murciano et al., 2007; Nabrit, 1929) or a square of tissue is removed in the middle of the fin (Nabrit, 1929). To understand how zebrafish skeletal cells regenerate in situations comparable to injury in non-regenerating systems, we developed and described a new caudal fin regeneration assay based on a precise bone crush injury and compared it with the classical amputation model of epimorphic regeneration. This new injury model may have important clinical implications since it is more close to mammalian fracture repair, thus helping to elucidate the mechanisms underlying bone repair.

Results

Comparison of crush injury and classical epimorphic regeneration models in the same caudal fin

To investigate the regeneration abilities of the zebrafish caudal fin in response to bony ray damage without tissue removal, we developed a new injury method consisting of precise crushing of single bony rays. This new repair assay will be referred to as crush injury, in contrast to the classically used technique to study epimorphic regeneration, which involves partial amputation of the fin with tissue removal (see Materials and Methods for details).

To allow the comparison between the two regeneration processes in the same fin, we amputated part of the caudal fin and on the opposite side we crushed bones in several rays (Fig. 1A). Analysis of the fins that suffer the two types of damage reveals clear differences in the general tissue architecture: whereas the crush injury site was easily distinguishable (Fig. 1B,C, asterisks) the amputation plane was hardly visible (Fig. 1B, arrowhead) at 10 dpc (days post-crush injury) and 10 dpa (days post-amputation), respectively.

When the crush injury was inflicted, only the bony rays and the epidermis, approximately two segments distally and proximal to the crush injury site were affected whereas the inter-ray tissue was not affected (Fig. 1D). Interestingly, around the crushed region a structure morphologically similar to a callus formed, resembling what is present during mammalian fracture repair (Fig. 1E) (Schindeler et al., 2008). The histological stainings, Alizarin Red and Hematoxylin/Eosin, suggest that the callus is an uncalcified tissue, which may provide stability between the ends of the previously broken bony rays (Fig. 1D,F).

Molecular wound healing is similar after crush injury to after amputation

During initial stages of regeneration, the amputation injury stump is covered by a multi-layered epithelium that interacts with and guides the blastema during growth, patterning, and differentiation

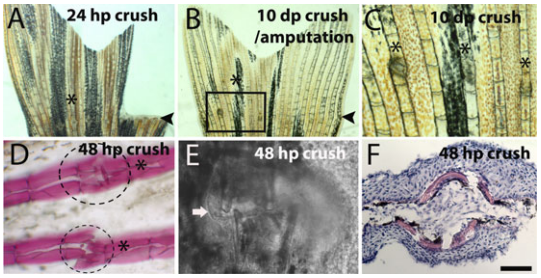

Fig. 1. Differences in tissue architecture after crush and amputation induced regeneration in the same caudal fin. (**A–C**) Bright filed image of a caudal fin after crush and cut at (A) 24 hpc/a and (B) 10 dpc/a. (C) Magnification of the inset in picture B. (**D**) Alizarin Red staining for bone matrix at 48 hpc; dashed lines indicates the region of callus formation that is not stained with Alizarin Red. (**E**) Bright field confocal image of 48 hpc injury site, the arrow highlights the callus structure. (**F**) Hematoxilin/Eosin staining in a transversal section of a 48 hpc ray. Arrowheads indicate the amputation plane and asterisks indicate crush injury area in A and B, and crush injury sites in C and D. Scale bar corresponds to 500 μm in A and B, 200 μm in C, 100 μm in D and 50 μm in E and F. (hpa – hours post-amputation; hpc – hours post-crush injury).

(Lee et al., 2009). In the context of crush injury we used immunofluorescence to evaluate for the presence of p63 protein, a member of the p53 family of transcription factors, used as structural marker for epidermis (Stewart et al., 2009). At 24 hpc, p63 was present at the epidermis that covers the crush injury site (Fig. 2A). However, this epidermis seems thicker at the crush injury site (Fig. 2A, asterisk) than at the neighbouring non-regenerating ray (Fig. 2A, arrow). These results, together with the histological staining shown in Fig. 1F, indicate that the crush callus results from a thickening of the epithelium.

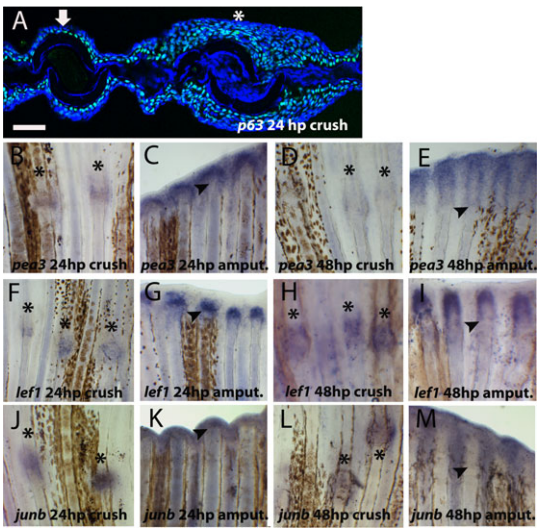

Fig. 2. Presence of wound healing marker genes after crush injury. (**A**) Immunohistochemistry for p63 (green) in 24 hpc transversal section of caudal fin. Blue represents DAPI positive nuclei. The arrow indicates an intact bony ray and the asterisk the site of crush injury. (**B–M**) Whole-mount *in situ* hybridization for mRNA of (B–E) *pea3* at (B) 24 hpc (C) 24 hpa (D) 48 hpc (E) 48 hpa; (F–I) *lef1* at (F) 24 hpc (G) 24 hpa (H) 48 hpc (I) 48 hpa; (J–M) *junb* at (J) 24 hpc (K) 24 hpa (L) 48 hpc (M) 48 hpa. Arrowheads indicate the amputation plane and asterisks indicate crush injury sites. Scale bar corresponds to 50 μm in A and 200 μm in B–M. (hpa – hours post-amputation; hpc – hours post-crush injury).

Besides covering the wound, the wound epidermis also synthesizes many secreted factors that mediate the communication between the blastema and the upper layers responsible for orchestrating the regeneration process (Stoick-Cooper et al., 2007). One of the major secreted factors is FGF, and one of its target genes *ETS-domain transcription factor pea3* (*pea3*) is strongly expressed at the basal epidermal layer since 24 after amputation (Fig. 2C) (Roehl and Nüsslein-Volhard, 2001). In contrast, at the same time point, in the crushed area *pea3* was expressed at very low levels (Fig. 2B). At 48 hpc *pea3* continues to be detected at low levels at the crush injury sites (Fig. 2D) when compared with amputated rays (Fig. 2E). Another classical wound epidermis marker is *lymphocyte enhancer binding factor 1* (*lef1*), a member of Wnt signalling pathway that is used to define the correct specification of the basal layer of the wound epidermis (Poss et al., 2000). At crush injury sites *lef1* mRNA was expressed at 24 hpc (Fig. 2F) but at lower levels than in the wound epidermis at the same time post-amputation (Fig. 2G). At 48 hpc the *lef1* expression seems to increase to levels comparable with amputated bony rays at the same time point (Fig. 2H,I). Additionally, we found a stress response gene, *jun B proto-oncogene (junb)*, expressed at 24 and 48 hpc (Fig. 2J–M) in the epidermis at crush injury sites, as it was after amputation (Ishida et al., 2010; Yoshinari et al., 2009). Together, these results indicate that the crush injury site was covered by a multilayered wound epidermis which shares the same molecular marker genes expressed during wound healing phase in the classical epimorphic regeneration. Although, *in situ* hybridization is not a quantitative technique, since the *in situ* was performed in the same sample, subjected to the exact same conditions, with exception of the type of injury, our results suggest that there is a delay in the activation of the FGF/WNT signalling pathways or/and that FGF/Wnt signalling is not so efficiently activated after crush as it is at early time points after amputation.

Blastema marker *msxb* expression was delayed after crush injury

Another characteristic feature of epimorphic regeneration is the formation of a specialized structure called blastema (Morgan, 1901), which contains the information to build the new organ or appendage. Using the described crush injury assay, we searched by *in situ* hybridization for the presence of *muscle segment homeobox B* (*msxb*), a marker for initial blastema formation (Nechiporuk and Keating, 2002). At 24 hpc *msxb* was not detected at crush injury sites (Fig. 3A), contrary to the amputation sites (Fig. 3B). However, at 48 hpc *msxb* was present in both injury models (Fig. 3C,D).

Next we investigated whether proliferation was also delayed, by doing immunohistochemistry using an antibody against PCNA. After amputation, the highest proliferation rate occurs at 48 hpa in blastema cells (Fig. 3F) but at this same time-point after crush there are comparatively less cell proliferation (Fig. 3E). These results further suggest that the formation of the blastema and initiation of proliferation were delayed after crush injury, when compared with epimorphic regeneration after amputation.

Differentiation of new skeletal cells is slow after crush injury

Our expression analysis results show that the timing of activation of the *msxb* blastema marker is delayed after crush injury. To investigate whether the expression of skeletogenesis specification

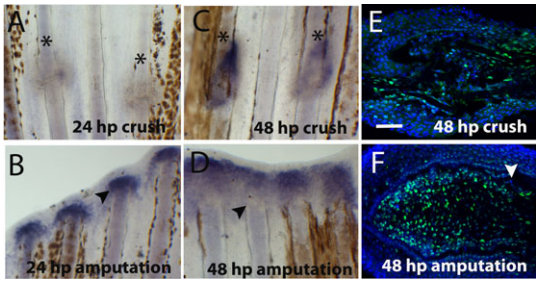

Fig. 3. Blastema marker, *msxb*, and proliferation after crush injury. (**A–D**) Whole-mount *in situ* hybridization for *msxb* mRNA at (A) 24 hpc (B) 24 hpa (C) 48 hpc (D) 48 hpa. Immunohistochemistry for the proliferation marker PCNA (green) at (**E**) 48 hpc around the crush injury site and (**F**) 48 hpa blastema (distal region is to the left and proximal to the right). DAPI (blue) is staining the nuclei. Arrowheads indicate the amputation plane and asterisks indicate crush injury sites. Scale bar corresponds to 100 µm. (hpa – hours post-amputation; hpc – hours post-crush injury).

genes was also delayed, we searched for an early skeletogenesis marker *osterix* (*osx*), a marker of the intermediate stages of skeletogenesis *collagen 1 (colI)*, and also a late differentiation marker involved in mineralisation, *osteonectin (osn)* at 24 and 48 hpc by *in situ* hybridization (Fig. 4A–L). None of the tested genes were expressed at 24 hpc by contrast to their expression after amputation (Fig. 4A,B,E,F,I,J). Later, at 48 hpc all these genes were expressed at the injury sites, reaching similar levels to the blastema expression after amputation (Fig. 4C,D,G,H,K,L).

To evaluate whether this delayed gene expression also led to a delay in the differentiation of the new bone tissue, we performed immunofluorescence using Anti-Zns5 antibody to detect deposition of skeletal cells after crush injury. This antibody labels bone cells at any stage of their differentiation (Johnson and Weston, 1995). At 24 hpc, at the injury site the two bone pieces of the same hemisegment were still apart, we could not detect any Zns5-positive cell at the crush injury site (Fig. 5A, arrow),

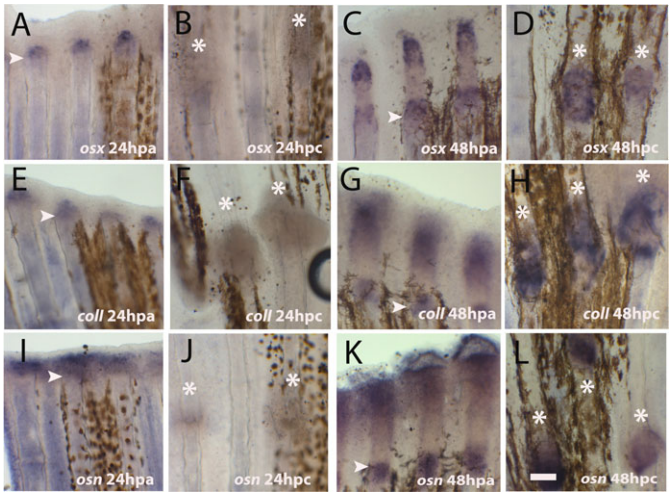

Fig. 4. Expression of skeletogenesis genes after crush injury. (**A–L**) Whole mount *in situ* hybridization for mRNA detection of (A–D) *osterix* at (A) 24 hpa; (B) 24 hpc (C) 48 hpa (D) 48 hpc; (E–H) *collagen I* at (E) 24 hpa (F) 24 dpc (G) 48 hpa (H) 48 hpc; (I–L) *osteonectin* at (I) 24 hpa (J) 24 hpc (K) 48 hpa (L) 48 hpc. Arrowheads indicate the amputation plane and asterisks indicate crush injury sites. Scale bar corresponds to 100 µm in all panels. (hpa – hours post-amputation; hpc – hours post-crush injury).

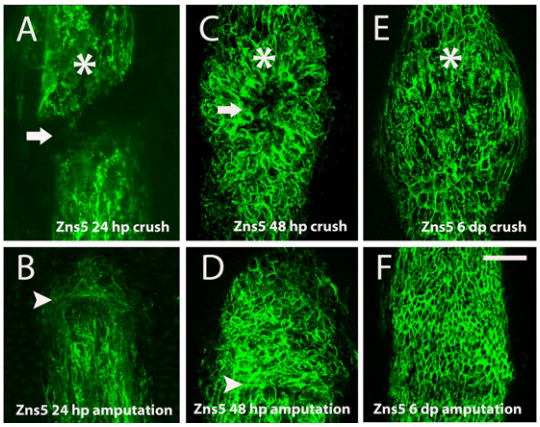

Fig. 5. Skeletal cell deposition was delayed and patterning was affected after crush injury. (**A–F**) Immunohistochemistry with the antibody anti-Zns5 to detect skeletal cells. (A) 24 hpc, the arrow highlights the lack of bone cells deposition (B) 24 hpa (C) 48 dpc (D) 48 hpa (E) 6 dpc (F) 6 dpa, near the amputation plane. Arrowheads indicate the amputation plane and asterisks indicate crush injury sites. Scale bar corresponds to 50 μm in all panels. (hpa – hours post-amputation; hpc – hours post-crush injury).

whereas after amputation at this time-point Zns5-positive cells were already detected at the newly formed blastema (Fig. 5B). At 48 hpc, skeletal cells were present at the crush injury site (Fig. 5C), as it happens at the 48 hpa blastema (Fig. 5D). Interestingly, the pattern of newly formed bone cells after crush injury seems to be different from the pattern that is observed after amputation; the bony ray structure gets rounded specifically at the crushed area (Fig. 5C,E). It seems that skeletal cells are being deposited both from the distal and proximal zones around the crush injury site from the periphery to the center of the ray (Fig. 5C, arrow). Such process of cell deposition could lead to a mispatterned bone tissue in comparison with a fully regenerated bony ray at 6 dpa (compare Fig. 5E with Fig. 5F).

Together, these results suggest that new bone tissue was formed after crush injury but this process was delayed when compared with epimorphic regeneration after amputation. Moreover, the fact that bone patterning differs at later regeneration stages in the two studied injury models lead us to investigate the hypothesis of prolonged bone repair (compare Fig. 5E with Fig. 5F). For this we checked by *in situ* hybridization for expression of *osteopontin*, a gene encoding a bone matrix protein that is known to be upregulated during bone remodelling, in mammals (Nomura and Takano-Yamamoto, 2000). Both at 24 and 48 hpc, *ostepontin* was detected at crush injury sites as well as in regenerating blastemas (Fig. 6A–D). At later stages, 6 dpc/a, in regenerating blastemas *osteopontin* expression was very low (Fig. 6E) in comparison to crush injury sites (Fig. 6F), further supporting the notion that bone repair was ongoing. Moreover, at 6 dpc Tenascin C, an extracellular matrix protein, indicative of differences in adhesion and migratory properties of cells (Jaźwińska et al., 2007; Chablais and Jazwinska, 2010) was still expressed at crush injury sites (Fig. 6G), whereas after amputation is it expressed at the first days of regeneration. At 24 hpa Tenascin C staining is strongly expressed in cells of the first segment below the amputation plan and in some blastema cells (Fig. 6H), but its expression is reduced at 48 hpa (Fig. 6J) and is very low at 72 hpa (Fig. 6K). After this stage we could not detect Tenascin C

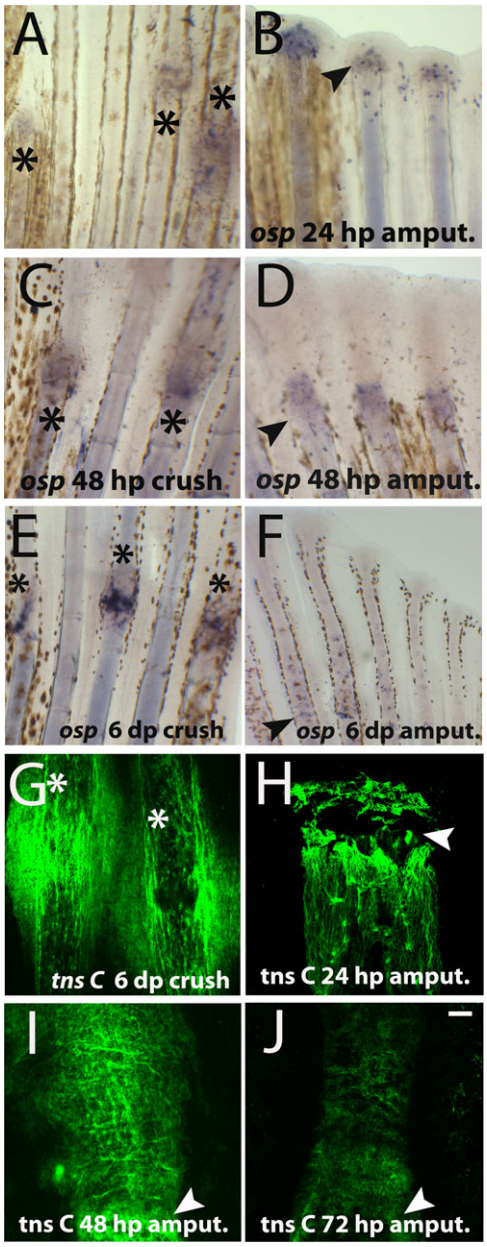

Fig. 6. Bone was undergoing repair 6 days post-crush injury. (**A–F**) Whole mount *in situ* hybridization for *osteopontin* mRNA. (A) 24 hpc (B) 24 hpa (C) 48 hpc (D) 48 hpa (E) 6 dpa (F) 6 dpc. (**G–J**) Whole mount immunofluorescense for Tenascin C at crush injury sites 6 dpc. Arrowheads indicate the amputation plane and asterisks indicate crush injury sites. Scale bar corresponds to 100 μm in all panels. (hpa – hours post-amputation; hpc – hours post-crush injury).

expression in the regenerating fin. All together, these data suggest that at late regenerative stages bone tissue was still undergoing a repair process at crush injury sites.

Blood vessels are affected by crush injury

Along with bone patterning alteration at later regeneration stages, we searched for other tissues types in the fin that could be also affected by crush injury. Blood vessels are found in close apposition to the fin ray, with arteries running inside the ray and veins lying along the outside. To evaluate the effect of crush injury on blood vessels, we used the Tg(*fli*:EGFP) zebrafish

transgenic line, as a reporter for endothelial cells (Lawson and Weinstein, 2002). At 24 hpc, the blood vessels were still disrupted (Fig. 7A). Noteworthy, only the main artery and not the veins in the intra-ray tissue, was damaged (Fig. 7A, arrow). After amputation, at 24 hpa the vessels were already undergoing anastomosis (Fig. 7B) (Huang et al., 2003). Interestingly, at 6 dpc we detected over-branching of the blood vessels (Fig. 7C) at crush injury sites, what differs from the regenerating blood vessels at the same time point after amputation (Fig. 7D).

Intra-ray nerves also run along the outside of the bone thus we also investigated whether the nerve fibers were affected by the crush injury. To visualize nerve fibers, we used the Anti-acetylated-Tubulin antibody (Kumar et al., 2007). At 24 hpc the bundle of intra-ray nerve fibers was perturbed (Fig. 7E), as well as after amputation (Fig. 7F). At 6 dpc reinnervation was completely reestablished (Fig. 7G) in comparison with the same time-point after amputation (Fig. 7H). However, after crush injury some nerve fibers at the intra-ray space seem deviated, possibly due to physical constraints. Together, our data demonstrate that at later stages blood vessels and skeletal cells are mispatterned at the crush injury sites, whereas nerve fibers recover the pre-injury pattern.

Discussion

Regeneration after crush injury is delayed when compared with amputation but both share similar molecular mechanisms

In this work we aimed to establish a new zebrafish bone repair assay comparable to mammalian bone fracture repair. The crush injury assay can be easily compared with regeneration after amputation (classical model) because we can perform both assays in the same caudal fin. The major difference between crush injury and regeneration after amputation is the type of injury applied. In the crush model, tissues suffer a less dramatic mechanical trauma because they remain in the same place, whereas after amputation the tissues are completely removed. We speculate that the surrounding tissues can participate in the overall morphogenesis of a structure regenerating after crush injury. Indeed, Tenascin C and PCNA-positive cells were present both in proximal and distal areas around the crush injury site, which might indicate that cells from both locations could participate in the repair process in this model.

The formation of a wound epidermis is critical to the success of the regenerative process. First, this multi-layered epithelium covers the wound to avoid infection. Secondly, wound epidermis secrets factors that orchestrate and guide the blastema during growth, patterning, and differentiation (Lee et al., 2009). Our p63 expression data suggest that the wound epidermis formed after crush injury is also multilayered and expresses wound epidermis markers such as *lef1* and *pea3*, at 24 hpc but at lower levels when compared with regeneration after amputation. One can speculate that these differences in expression reflect differences on tissue structure. Indeed, after crush injury there is a formation of a structure similar to the callus, which is normally formed where there is tissue motility around the fracture site during mammalian fracture repair. This callus-like structure, mostly epithelial, is not present in regenerating caudal fin after amputation. Thus, the formation of this callus possibly could lead to a less efficient and/or delayed activation of FGF/WNT signalling after crush injury than after amputation.

Nevertheless, the presence of characteristic wound epidermis markers, *lef1* and *pea3*, at 24 hpc indicates that the wound epidermis was specified correctly after crush injury, which is crucial for the success of the regenerative process (Poss et al., 2000; Lee et al., 2009). Moreover, the low levels of expression of these factors at 24 hpc could justify the fact that all the subsequent gene expression was delayed. For instance, *msxb*, a blastema marker was only expressed later at 48 hpc. Like *msxb*, expression of skeletogenic genes (*osterix*, *collagen1* and *osteonectin*) was also delayed and sequentially *de novo* bone formation happens at 48 hpc.

Altogether, our results indicate that the regenerative process after crush injury and after amputation share the same molecular program but when the injury is inflicted by crush the regeneration onset seems delayed and maintained for longer, possibly due to differences in epidermis tissue architecture after crush injury.

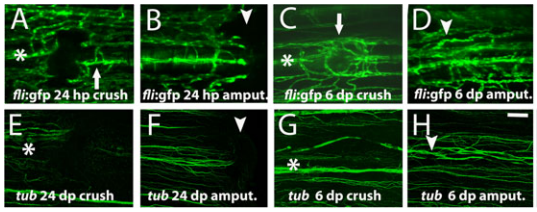

Fig. 7. Blood vessels structure was compromised, whereas nerve bundles were not after crush injury. (**A–D**) Imaging of the transgenic line *fli*:EGFP that labels the endothelial cells at (A) 24 hpc, arrow indicates the main bony ray artery (B) 24 hpa (C) 6 dpc, arrow highlights the blood vessels mispatterning (D) 6 dpa. (**E–H**) Immunohistochemistry with the antibody anti-acetylated Tubulin to detect nerve fibres at (E) 24 hpc (F) 24 hpa (G) 6 dpc (H) 6 dpa. Arrowheads indicate the amputation plane and asterisks indicate crush injury sites. Scale bar corresponds to 100 µm in all panels. (hpa – hours post-amputation; hpc – hours post-crush injury; dpa – days post-amputation; dpc – days post-crush injury).

Bone and blood vessel patterning was affected after crush injury

Another difference between the two repair processes that we have studied was the morphological aspect of the bony rays. Several days after crush injury it was still possible to identify the injury sites, whereas in the same fin the amputation plane was hardly visible. This is due to the fact that bone tissue remains mispatterned at later regenerative stages after crush injury. At the crush injury site after 6 dpc the skeletal cells instead of being aligned in a distal to proximal position, as after amputation, seem to be radially oriented. It is known that bone tissue is extremely sensitive to the type of mechanical trauma inflicted (Allori et al., 2008), thus we can speculate that after crush injury different signals are activated and the tissue reacts differently to the distinct physical/mechanical constraints.

Previous studies in zebrafish showed that bone tissue was mispatterned when the vascular plexus pattern was abnormal, demonstrating that blood vessels play an important role in the patterning of bony rays in zebrafish caudal fins (Huang et al., 2009). After crush injury, this interaction between blood vessels and bone is also an hypothesis because along with bone tissue being mispatterned blood vessels also seem to be abnormally reconnected. Indeed, this phenotype resembles the *persistent plexus* (*prp*) mutant, in which the vessels and bony ray are also wrongly patterned (Huang et al., 2009). The signal(s) that is behind this interaction between bone tissue and blood vessels is currently unknown.

Additionally, we examined nerve fibers and we found that its pattern was relatively normal after crush injury, thus they do not

seem to follow the same cues as blood vessels or skeletal cells. Along with the recent literature (Huang et al., 2009; Huang et al., 2003) our data suggest that after amputation the vascular pattern (and not the nerves) guide the osteoblast pattern in fins after crush injury, consequently bone defects might be a secondary phenotype to blood vessel mispatterning.

Prolonged repair may impair perfect bone re-patterning

Our data suggest that several aspects of bone repair take significantly longer in the crush assay than in regeneration after amputation. The extracellular matrix component Tenascin C is involved in the regulation of cell adhesion and has been shown to instruct cell shape, migration and proliferation during early regeneration stages after amputation (Yu et al., 2011; Jaźwińska et al., 2007; Chablais and Jazwinska, 2010), during muscle regeneration (Calve et al., 2010) and after cryoinjury of zebrafish heart (Chablais et al., 2011). However, Tenascin C expression disappears in mature tissues (Chablais and Jazwinska, 2010), thus the fact that it is still detected at 6 dpc is indicative that bone repair processes are active at crush injury sites for longer than after amputation. In addition, a tissue remodelling marker, *osteopontin* has also a prolonged expression after crush injury. Osteopontin is a major non-collagenous bone matrix protein that plays an important role in bone formation and resorption. In mammals, shortly following fracture, *osteopontin* is markedly upregulated in osteoblasts, suggesting that it is involved in the immediate recruitment of cells for fracture healing and bone remodeling (Denhardt and Guo, 1993). We can speculate that prolonged repair may lead to imperfect bone re-patterning as we observe in the crush assay.

This work allowed us to explore a new model of caudal fin injury more similar to mammalian fracture repair as it relies on tissue crush injury instead of tissue removal. Interestingly, our data show that the repaired tissue is mispatterned, making this assay a potential better platform for skeletal studies, for example to test new therapeutics to accelerate bone repair and re-patterning.

Materials and Methods

Fish manipulation and amputation

Wild-type AB strain adult zebrafish, *Danio rerio*, (3–6 months old) were anesthetized in 0.1% tricaine (MS-222 ethyl-m-aminobenzoate, Sigma-Aldrich) and the caudal fins amputated using a scalpel or crushed using forceps. Regeneration was then allowed to proceed until defined time points at 33℃. Fish were then anesthetized and fins collected for further analysis. The transgenic line used was Tg(*fli*:EGFP) (reported by Lawson and Weinstein, 2002).

Skeletal staining

Collected fins were fixed 100% ethanol (EtOH). The EtOH was changed after 20 minutes for fresh EtOH and incubated for at least 1–2 days at room temperature. For the alizarin red staining, incubation of the samples was done in 50 mg/L Alizarin Red S (Gurr Searle Diagnostic, UK) in 2% KOH (pH 4,1–4.3; Sigma-Aldrich), during 2–8 hours at room temperature. At this step the bone was stained in red. Next, the samples were cleared by the incubation with 2% KOH at room temperature for 10 minutes, until the soft tissues were degraded and the skeletal elements completely visible. To stop the reaction the 2% KOH solution was replaced by another solution with 2% KOH and 25% glycerol (Sigma-Aldrich). The samples were kept in this solution at room temperature until complete equilibration of it with the glycerol. For storage we use a 100% glycerol solution.

Hematoxylin/Eosin staining

Sections were washed in water during 5 minutes and stained in Harri's Hematoxylin (Sigma-Aldrich) for another 5 minutes. After a brief wash in water, sections were immersed 3 times in 1% Chloridric acid (Merck), washed with water for 5 minutes and immersed in 70% Ethanol. Then samples were stained with Eosin solution (Sigma-Aldrich) by immersing the sections 4 times and then passed though Ethanol series from 70 to 100% dilution. For observation the sections were mounted in Xilol (Klinipath, The Netherlands).

In situ hybridization

In situ hybridization for mRNA detection was carried out as described by Sousa et al., 2011. Details for RNA probes for *osterix (sp7)*, *osteonectin (osn)* and *collagen (col1a2)* genes were (described by Li et al., 2009). *Lef1* probe was prepared from the EST clone 998C 1015213Q1 (ImaGenes, Source BioScience, UK) and *junb* probe was cloned using forward primer 5′ATGTCAACAAAAATGGAGCAAC3′ and reverse primer 5′CTAAAACGACTTGATCTTGGGC3′.

Immunofluorescence

The immunofluorescence protocol was performed as described by Sousa et al., 2011. The primary antibodies used were the monoclonal anti-Zns5 antibody to mark scleroblasts (ZIRC 011604, USA), anti-Tenascin C (137.T2550-23, US BIOLOGICAL, MA, USA), anti-p63 antibody (06.570, Santa Cruz Biotechnology, CA, USA), anti-acetylated Tubulin (T-7451, Sigma-Aldrich) and anti-PCNA (F2007, Santa Cruz Biotechnology, CA, USA).

Acknowledgements

We thank the fish facility staff, Lara Carvalho and Susana Ponte, for animal care support. We thank Rita Fior, Leonor Saúde and Henry Roehl for reading the manuscript and for insightful discussions and Rita Mateus for reagents. This work was supported by the Fundação para a Ciência e Tecnologia (FCT), Portugal [PTDC/SAU-OBD/100200/2008, PTDC/SAU-OBD/73112/2006, and SFRH/BD/32952/2006 to S.S].

Competing Interests

The authors have no competing interests to declare.

References

Akimenko, M.-A., Marí-Beffa, M., Becerra, J. and Géraudie, J. (2003). Old questions, new tools, and some answers to the mystery of fin regeneration. *Dev. Dyn.* **226**, 190-201.

Allori, A. C., Sailon, A. M., Pan, J. H. and Warren, S. M. (2008). Biological basis of bone formation, remodeling, and repair-part III: biomechanical forces. *Tissue Eng. Part B Rev.* **14**, 285-293.

Calve, S., Odelberg, S. J. and Simon, H.-G. (2010). A transitional extracellular matrix instructs cell behavior during muscle regeneration. *Dev. Biol.* **344**, 259-271.

Chablais, F. and Jazwinska, A. (2010). IGF signaling between blastema and wound epidermis is required for fin regeneration. *Development* **137**, 871-879.

Chablais, F., Veit, J., Rainer, G. and Jaźwińska, A. (2011). The zebrafish heart regenerates after cryoinjury-induced myocardial infarction. *BMC Dev. Biol.* **11**, 21.

Denhardt, D. T. and Guo, X. (1993). Osteopontin: a protein with diverse functions. *FASEB J.* **7**, 1475-1482.

Huang, C.-C., Lawson, N. D., Weinstein, B. M. and Johnson, S. L. (2003). *reg6* is required for branching morphogenesis during blood vessel regeneration in zebrafish caudal fins. *Dev. Biol.* **264**, 263-274.

Huang, C.-C., Wang, T.-C., Lin, B.-H., Wang, Y.-W., Johnson, S. L. and Yu, J. (2009). Collagen IX is required for the integrity of collagen II fibrils and the regulation of vascular plexus formation in Zebrafish caudal fins. *Dev. Biol.* **332**, 360-370.

Ishida, T., Nakajima, T., Kudo, A. and Kawakami, A. (2010). Phosphorylation of Junb family proteins by the Jun N-terminal kinase supports tissue regeneration in zebrafish. *Dev. Biol.* **340**, 468-479.

Jaźwińska, A., Badakov, R. and Keating, M. T. (2007). Activin-betaA signaling is required for zebrafish fin regeneration. *Curr. Biol.* **17**, 1390-1395.

Johnson, S. L. and Weston, J. A. (1995). Temperature-sensitive mutations that cause stage-specific defects in Zebrafish fin regeneration. *Genetics* **141**, 1583-1595.

Knopf, F., Hammond, C., Chekuru, A., Kurth, T., Hans, S., Weber, C. W., Mahatma, G., Fisher, S., Brand, M., Schulte-Merker, S. et al. (2011). Bone regenerates via dedifferentiation of osteoblasts in the zebrafish fin. *Dev. Cell* **20**, 713-724.

Kragl, M., Knapp, D., Nacu, E., Khattak, S., Maden, M., Epperlein, H. H. and Tanaka, E. M. (2009). Cells keep a memory of their tissue origin during axolotl limb regeneration. *Nature* **460**, 60-65.

Kumar, A., Godwin, J. W., Gates, P. B., Garza-Garcia, A. A. and Brockes, J. P. (2007). Molecular basis for the nerve dependence of limb regeneration in an adult vertebrate. *Science* **318**, 772-777.

Laforest, L., Brown, C. W., Poleo, G., Géraudie, J., Tada, M., Ekker, M. and Akimenko, M. A. (1998). Involvement of the sonic hedgehog, patched 1 and bmp2 genes in patterning of the zebrafish dermal fin rays. *Development* **125**, 4175-4184.

Lawson, N. D. and Weinstein, B. M. (2002). *In vivo* imaging of embryonic vascular development using transgenic zebrafish. *Dev. Biol.* **248**, 307-318.

Lee, Y., Hami, D., De Val, S., Kagermeier-Schenk, B., Wills, A. A., Black, B. L., Weidinger, G. and Poss, K. D. (2009). Maintenance of blastemal proliferation by functionally diverse epidermis in regenerating zebrafish fins. *Dev. Biol.* **331**, 270-280.

Li, N., Felber, K., Elks, P., Croucher, P. and Roehl, H. H. (2009). Tracking gene expression during zebrafish osteoblast differentiation. *Dev. Dyn.* **238**, 459-466.

Mackie, E. J. (1994). Tenascin in connective tissue development and pathogenesis. *Perspect. Dev. Neurobiol.* **2**, 125-132.

Maes, C., Kobayashi, T., Selig, M. K., Torrekens, S., Roth, S. I., Mackem, S., Carmeliet, G. and Kronenberg, H. M. (2010). Osteoblast precursors, but not mature osteoblasts, move into developing and fractured bones along with invading blood vessels. *Dev. Cell* **19**, 329-344.

Morgan, T. H. (1901) *Regeneration*. New York: Macmillan & Co.

Murciano, C., Pérez-Claros, J., Smith, A., Avaron, F., Fernández, T. D., Durán, I., Ruiz-Sánchez, J., García, F., Becerra, J., Akimenko, M.-A. et al. (2007). Position dependence of hemiray morphogenesis during tail fin regeneration in *Danio rerio*. *Dev. Biol.* **312**, 272-283.

Nabrit, S. M. (1929). The role of the fin rays in the regeneration in the tail-fins of fishes: in Fundulus and Goldfish. *Biol. Bull.* **56**, 235-266.

Nechiporuk, A. and Keating, M. T. (2002). A proliferation gradient between proximal and msxb-expressing distal blastema directs zebrafish fin regeneration. *Development* **129**, 2607-2617.

Nomura, S. and Takano-Yamamoto, T. (2000). Molecular events caused by mechanical stress in bone. *Matrix Biol.* **19**, 91-96.

Poss, K. D. (2010). Advances in understanding tissue regenerative capacity and mechanisms in animals. *Nat. Rev. Genet.* **11**, 710-722.

Poss, K. D., Shen, J. and Keating, M. T. (2000). Induction of lef1 during zebrafish fin regeneration. *Dev. Dyn.* **219**, 282-286.

Roehl, H. and Nüsslein-Volhard, C. (2001). Zebrafish pea3 and erm are general targets of FGF8 signaling. *Curr. Biol.* **11**, 503-507.

Schindeler, A., McDonald, M. M., Bokko, P. and Little, D. G. (2008). Bone remodeling during fracture repair: The cellular picture. *Semin. Cell Dev. Biol.* **19**, 459-466.

Sousa, S., Afonso, N., Bensimon-Brito, A., Fonseca, M., Simões, M., Leon, J., Roehl, H., Cancela, M. L. and Jacinto, A. (2011). Differentiated skeletal cells contribute to blastema formation during zebrafish fin regeneration. *Development* **138**, 3897-3905.

Stewart, S., Tsun, Z.-Y. and Izpisua Belmonte, J. C. (2009). A histone demethylase is necessary for regeneration in zebrafish. *Proc. Natl. Acad. Sci. USA* **106**, 19889-19894.

Stoick-Cooper, C. L., Moon, R. T. and Weidinger, G. (2007). Advances in signaling in vertebrate regeneration as a prelude to regenerative medicine. *Genes Dev.* **21**, 1292-1315.

Yoshinari, N., Ishida, T., Kudo, A. and Kawakami, A. (2009). Gene expression and functional analysis of zebrafish larval fin fold regeneration. *Dev. Biol.* **325**, 71-81.

Yu, Y.-M., Cristofanilli, M., Valiveti, A., Ma, L., Yoo, M., Morellini, F. and Schachner, M. (2011). The extracellular matrix glycoprotein tenascin-C promotes locomotor recovery after spinal cord injury in adult zebrafish. *Neuroscience* **183**, 238-250.